Soft Matter

A non-equilibrium state diagram for liquid/fluid/particle mixtures†

Sachin S. Velankar

The equilibrium structures of ternary oil/water/surfactant systems are often represented within a triangular composition diagram with various regions of the triangle corresponding to different equilibrium states. We transplant this idea to ternary liquid/fluid/particle systems that are far from equilibrium. Liquid/liquid/particle mixtures or liquid/gas/particle mixtures yield a wide diversity of morphologies including Pickering emulsions, bijels, pendular aggregates, spherical agglomerates, capillary suspensions, liquid marbles, powdered liquids, and particle-stabilized foams. This paper argues that such ternary liquid/fluid/particle mixtures can be unified into a non-equilibrium state diagram. What is common among all these systems is that the morphology results from an interplay between the preferential wettability of the particles, capillarity, and viscous forces encountered during mixing. Therefore all such systems share certain universal features, regardless of the details of the particles or fluids used. These features guide the construction of a non-equilibrium state diagram which takes the form of a triangular prism, where each triangular cross-section of the prism corresponds to a different relative affinity of the particles towards the two fluids. We classify the prism into regions in which the various morphologies appear and also emphasize the major difference between systems in which the particles are fully-wetted by one of the fluids *vs.* partially-wetted by both fluids. We also discuss how the state diagram may change with mixing intensity or with interparticle attractions.

1. Introduction

Ternary mixtures composed of hydrocarbon oil, water, and surfactant show rich phase behavior including multiphase equilibrium, microemulsion phases, or liquid crystalline phases. Exhaustive studies of such mixtures have resulted in detailed ternary phase diagrams showing the equilibrium structures, phase transitions, and tie lines connecting coexisting phases. Such a ternary diagram may also be "extruded" into a triangular prism using some relevant parameter, *e.g.* temperature, pH, electrolyte concentration, as the axis of the prism. Beautifully detailed examples of prismatic phase diagrams have been constructed.[1,2] Fig. S1 in the ESI,† reproduces one such diagram from Leaver *et al.*[3] in which temperature-induced changes in phase behavior are represented within a triangular prism. Fig. S1 (ESI†) also reproduces a well-known diagram from Davis[2] showing schematics of the various microstructures. This research has also inspired other ternary phase diagrams that are variations on the same theme, *e.g.* with the oil being fluorinated, or one or both liquids being polymeric, or the surfactant being a block copolymer.[4–7]

Here we consider another class of ternary systems. These are composed of two immiscible fluids, often oil and water,

Department of Chemical Engineering, University of Pittsburgh, Pittsburgh,
PA 15261, USA. E-mail: velankar@pitt.edu; Tel: +1-412-624-9984
† Electronic supplementary information (ESI) available. See DOI: 10.1039/c5sm01901j

although sometimes one of the fluids may be air or a molten polymer. The third component is not a molecular surfactant, but instead, a particulate species. Such ternary mixtures can also show a wide diversity of structures including liquid marbles, spherical agglomerates, armored drops, particle-stabilized foams, bijels, suspensions with capillary interactions, and Pickering emulsions. In some of these cases, the particles reside within one of the bulk fluid phases. In others, the particles adsorb at the interface between the two fluids and behave somewhat like conventional surfactants.[8] It is therefore natural to ask whether the diverse morphologies that have been noted in such systems can also be catalogued on a ternary prism analogous to ESI,† Fig. S1. Unlike oil/water/surfactant mixtures, liquid/fluid/particle mixtures are generally not in thermodynamic equilibrium, although rare examples of true equilibrium have been noted.[9] Accordingly an *equilibrium* phase diagram is not possible. Nevertheless, the ESI,† accompanying this article shows that mixing three components (two fluid, one particulate), yields specific morphologies that are rather insensitive to the details the fluids, particle sizes, or the mixing operation. This suggests that a *non-equilibrium* state diagram may exist which unifies the microstructure-composition relationship across a diverse variety of liquid/fluid/particle mixtures. In previous publications, we have used the idea of a state diagram to guide experiments.[10–12] Nonomura and Kobayashi[13] have used the same motif to represent results of phase inversion

of Pickering emulsions. Recently, Koos[14] has assigned different regions of the ternary composition space to different microstructures. This Highlight seeks to construct a detailed state diagram of liquid/fluid/particle mixtures along with a discussion of the factors governing structure formation.

This article is organized as follows. Section 2 defines the parameter space of the ternary prism within which a state diagram can be constructed. Section 3 summarizes the morphologies commonly observed in various regions of the parameter space. Exemplary cases informing Section 3 are reproduced in the ESI.† They show that a wide variety of systems with diverse fluids (oil, water, molten plastics, air), and a wide range of particle sizes (from 50 nm to mm) display similar behavior, and thus argue in favor of a state diagram with widespread validity. Section 4 constructs such a diagram for one specific system and discusses the factors governing structure formation. An important goal is to emphasize that the microstructure of liquid/fluid/particle systems results from an interplay between three physical "forces": viscous forces generated during mixing, capillarity (i.e. the tendency to minimize interfacial area between the two fluids), and wettability (i.e. the affinity of the particles for one or both fluids). These three forces guarantee certain universal features, e.g. that a phase that fully-wets the particles is certain to develop a yield stress beyond some particle loading, or that particles that are partially-wetted by both fluids adsorb strongly at liquid/fluid interfaces. These features, which are generic to all liquid/fluid/particle mixtures, then pin down the structural transitions in the state diagram. The state diagram of Section 4 makes some simplifications, e.g. that the particles are approximately hard, polydisperse, spheres, or that the two fluids are viscosity-matched. Section 5 comments on how the transitions are expected to shift when these assumptions relaxed.

2. Parameter space in a ternary prism

Fig. 1a illustrates a ternary composition diagram for a mixture of particles (p) and two immiscible fluids (A and B). In this diagram and throughout this paper, composition is represented through the volume fractions ϕ_A, ϕ_B and ϕ_p. In the white triangle adjoining the lower edge, particles are the most dilute of the three species. Nominally, one may classify this region as an emulsion. In the two colored triangles flanking the white triangle, one of the fluid species is more dilute than the particles, whereas in the upper gray quadrilateral, both the fluids are more dilute than the particles. All three of these shaded regions are dubbed suspensions. It must be emphasized that this distinction between emulsions and suspensions is just a matter of nomenclature; the boundaries separating these regions are not necessarily associated with abrupt structural transitions. Nevertheless this distinction is convenient because much of the experimental literature is near the edges of the triangle where it is natural to think of the ternary system as either "an emulsion with added particles" or as a "suspension with added drops". A portion of this parameter space where particles are highly concentrated is difficult to access, e.g. hard sphere particulate systems often become glassy or solid-like for $\phi_p > 0.5$, and even realizing a macroscopically-homogeneous mixture may be difficult in this region. Thus it is only in the lower portion of this triangle that a structural classification is meaningful.

Before proceeding, we note that the affinity of the particles towards the two fluids is a crucial determinant of structure. In particular, this paper emphasizes major differences between the cases when the particles are fully-wetted by one fluid vs. partially-wetted by both fluids. This dependence on particle affinity can be represented by extruding the ternary composition diagram into a prism (Fig. 1b), with the vertical direction being the wettability of the particles towards the two phases. Analogous to oil/water/surfactant systems,[1–3] one may conduct experiments within specific slices, e.g. Fig. 1b, of this prism.

The particle wettability can be quantified by a three-phase contact angle, here defined as the contact angle measured through the B phase (Fig. 1c). It must be acknowledged however, that it is difficult to quantify contact angles of small particles. Methods to measure or estimate contact angles on particle surfaces
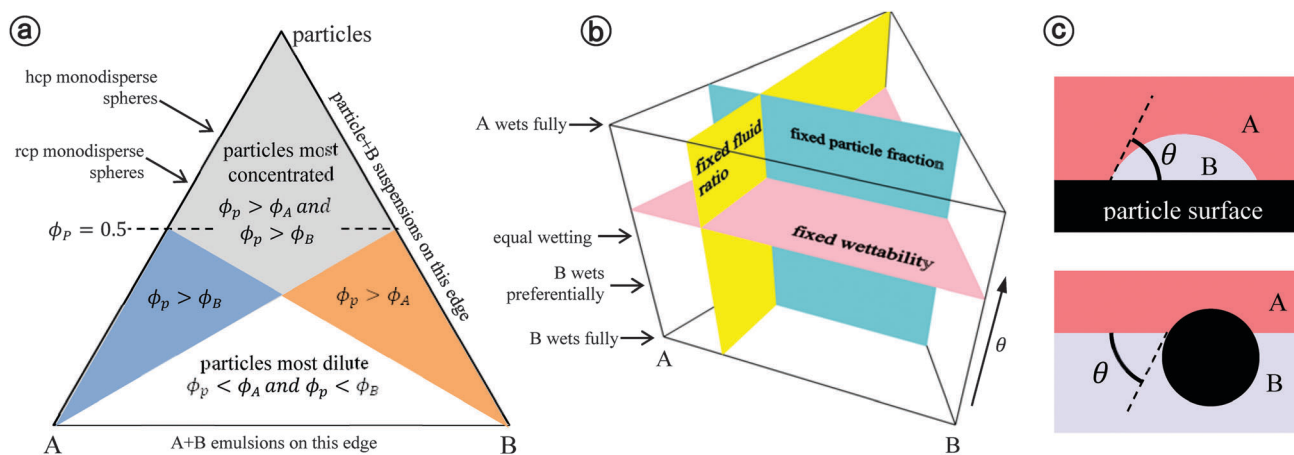

Fig. 1 (a) Schematic of ternary composition diagram marking various regions. (b) Ternary prism as particle wettability is changed. Various cross sections of the prism are labeled. (c) Two equivalent definitions of contact angle. Upper shows a drop on the surface of a solid surface with the contact angle measured through the B phase. Lower shows a spherical particle at the A/B interface making the same contact angle measured through the B phase.

are experimentally-demanding or subject to uncertainties;[15–21] there may also be significant hysteresis in contact angles and significant variability in contact angles within a single batch of particles.[22,23] Thus, in this paper, contact angles are taken as a measure of relative wettability; $\theta < 90°$ implies preferential-wetting of the particles by B, $\theta > 90°$ implies preferential wettability by the A fluid, and $\theta = 90°$ indicates equal-wetting by A and B.

3. Brief summary of structural transitions along trajectories in the parameter space

The ESI,† reviews past literature on ternary liquid/fluid/particle systems. Fig. S3–S19 (ESI†) were selected from the literature to highlight the various microstructures commonly seen in such systems, and more importantly, how these microstructures change as the ternary composition is changed. The systems are diverse. The fluids may be water, air, oil, or highly viscous molten polymers. The particles sizes range from less than 0.1 μm to over 100 μm, and include both monodisperse as well as polydisperse particles. The mixing methods are varied: e.g. a tumbler mixer for a wet granular material, a twin screw extruder for a filled polymer blend, a homogenizer for oil/water mixtures, or even simple shaking by hand. Different physical forces appear in different systems, e.g. electrostatic interactions are important in water-containing systems but not otherwise; gravitational effects are important in air-containing systems but not otherwise; air/liquid systems always have a severe viscosity mismatch, whereas oil/water or polymeric systems may not; viscoelasticity may be important in polymeric systems but not otherwise; frictional forces may be important if the particles are large but not otherwise. Across all such systems,
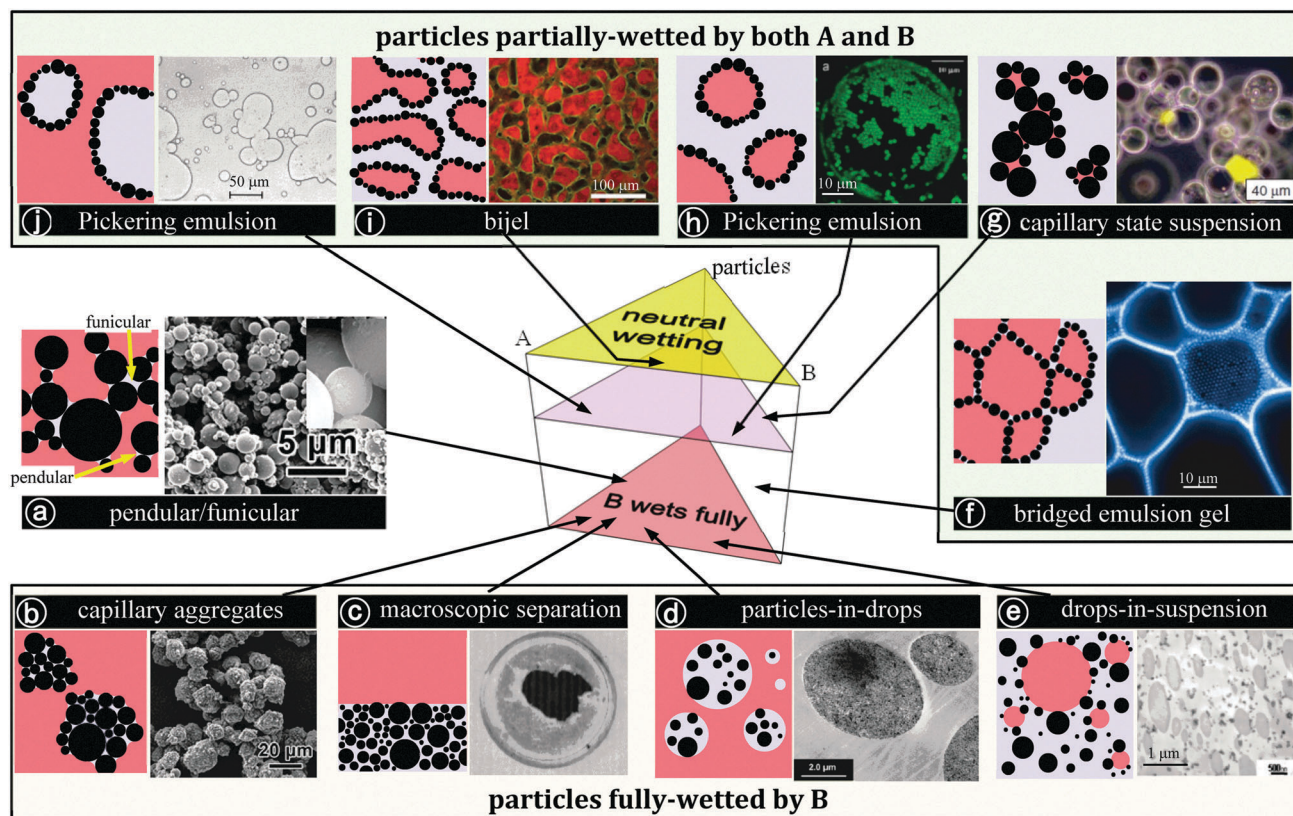

Fig. 2 Morphologies in various regions of the state prism for liquid/liquid/particle mixtures. Note that the prism does not extend up to full wettability by A, i.e. only the lower portion of the prism in Fig. 1c is shown. (a) Pendular morphology,[12,27] (b) capillary aggregates,[12] (c) macroscopically-separated system,[30] (d) particles-in-drops morphology,[57] (e) drops and particles both suspended in a matrix;[58] (f) bridged Pickering emulsion gels,[38] (g) capillary state suspension,[21] (h) Pickering emulsion,[59] (i) bijel,[54] (j) Pickering emulsion. Structures (b−e) require that the particles be fully-wetted by fluid B (shaded in light blue). Structures (f−j) require that particles be partially-wetted by both phases. The pendular/funicular structure, (a) can appear at both full as well as partial wettability. All images are reproduced from the literature as follows. (a and b) Reproduced from Domenech and Velankar, Soft matter, 2015, 11, 1500[12] with permission from The Royal Society of Chemistry. (c) Reproduced from Sirianni et al., Can. J. Chem. Eng., 1969, 47, 166[30] with permission from Wiley; all rights reserved. (d) Reprinted from Cai et al., Polymer, 2012, 53, 259,[57] Copyright (2012), with permission from Elsevier. (e) Reproduced from Lee et al., Macromol. Mater. Eng., 2012, 297, 95[58] with permission from Wiley; All rights reserved. (f) Reprinted with permission from Lee et al., Langmuir, 2012, 28, 3085,[38] Copyright (2011) American Chemical Society (g) From Koos and N. Willenbacher, Science, 2011, 331, 897.[21] Reprinted with permission from AAAS (h) reprinted with permission from Tarimala and Dai, Langmuir, 2004, 20, 3492,[59] Copyright (2004) American Chemical Society. (i) Reproduced from Tavacoli et al., Adv. Funct. Mater., 2011, 21, 2020[54] with permission from Wiley; All rights reserved. (j) Reprinted with permission from Binks and Lumsdon, Langmuir, 2000, 16, 2539,[60] Copyright (2000) American Chemical Society.

two common themes stand out. The first is that there are significant qualitative differences between the microstructures appearing when particles are fully-wetted by one of the phases *vs.* partially-wetted by both phases. The second is that – once these differences in wettability are taken into account – similar morphologies appear in similar regions of composition space regardless of all of the other differences noted above. These observations motivate the central claim of this paper: by treating the particle wettability as a parameter, all these mixtures can be classified on a single state diagram constructed within the triangular prism of Fig. 1c.

Fig. 2 illustrates such a classification along with schematic versions of the morphologies observed in various regions of the prism, and with typical experimental examples of such morphologies. Fig. 2 corresponds to liquid/liquid/particle mixtures; an analogous diagram for water/air/particle mixtures is shown in ESI,† Fig. S2. The location of each structure indicated by the arrows in Fig. 2 and Fig. S2 (ESI†) is intended to be approximate: depending on the details, any particular structure may appear at a somewhat different location within the prism, or across a wider range of locations, than indicated. Sections 3.1–3.3 summarize the main characteristics of Fig. 2 and Fig. S2; details and citations are provided in the ESI.† The following Section 4 will then construct a quantitative state diagram to capture these observations.

3.1. Liquid/liquid mixtures with fully-wettable particles

"Fully" wettable in this context means that the particles can be completely engulfed by phase B. That does not necessarily require that the contact angle with respect to B be zero; particles can be fully-engulfed even if the contact angle is small but not zero. With fully-wettable particles, the following sequence of transitions appears as one starts on the A–p edge of the triangle and traverses to the right. Adding a small amount of wetting fluid B to particles dispersed in the non-wetting fluid leads to the formation of pendular aggregates, *i.e.* particles joined pair-wise by menisci of B (Fig. 2a). With increasing amount of B the menisci coalesce, first leading to funicular aggregates, and then to full engulfment of some of the particles, corresponding to the formation of capillary aggregates (Fig. 2b). At wetting fluid loadings slightly exceeding that for capillary aggregates, large-scale separation occurs, the A phase (without any particles) and the B phase engulfing all the particles (Fig. 2c). With further increases in wetting fluid loading, a particles-in-drops morphology appears, *i.e.* an emulsion in which the B drops themselves contain particles (Fig. 2d). At sufficiently high loading of the wetting fluid, phase inversion occurs, with the particles now being suspended in the continuous phase B, dubbed drops-in-suspension (Fig. 2e). While oil/water systems show conventional phase inversion with the dispersed fluid becoming the continuous phase and *vice versa*, polymeric systems can show bicontinuous structures at intermediate liquid volume ratios.

3.2. Liquid/liquid mixtures with partially-wettable particles

"Partial" wetting in this context means that the liquid/liquid contact line cannot readily advance across the particle. Certainly full wetting can be forced to happen, *e.g.* a highly hydrophobic

particle will sink in water if it is sufficiently heavy. In many circumstances however, the particles are highly resistant to being completely engulfed by one of the phases. In such cases the following morphologies appear. In most of this section, B will be regarded as the preferentially-wetting fluid, *i.e.* $\theta < 90°$.

As long as θ is far less than 90°, one may still expect pendular or funicular structures (Fig. 2a) to form near the p–A edge of the triangle. However much of the rest of the composition space is occupied by particle-stabilized Pickering emulsions (Fig. 2h and j). Due to particle crowding at the interface, such emulsions are often characterized by non-spherical drop shapes. As noted in the ESI,† the phase that preferentially-wets the particles usually becomes the continuous phase, *i.e.* in most Pickering emulsions, particles protrude more out of the drops than into the drops. If θ is small (but not too close to zero) a remarkable morphology called a bridged Pickering emulsion gel can appear (Fig. 2f) in which each particle is shared by two drops of the less-wetting liquid A. Finally, if the less-wetting liquid A is at a very low loading, a related structure dubbed a capillary state suspension has been identified (Fig. 2g).

Under neutrally-wetting conditions ($\theta \approx 90°$) Pickering emulsions can still be formed, although sometimes they are reported to be unstable. Multiple emulsions, *i.e.* with a droplets within droplets, have also been noted. A noteworthy feature at $\theta \approx 90°$ is the possibility of a bijel, a bicontinuous morphology stabilized by a jammed monolayer of interfacially-adsorbed particles (Fig. 2i).

3.3. Mixtures in which one fluid is air

When one fluid is air, buoyancy/gravity effects are always important, and hence the three-phase composition cannot be controlled directly. Only the particle : liquid ratio can be specified; the system then "decides" how much air to entrain. Moreover, not all regions of composition space are accessible. For instance, it is not meaningful to think of a mixture of sand, water, and air in a 10 : 1 : 100 proportion; such a mixture will collapse into a wet granular pile that incorporates relatively little air. A second, less important, feature is that the fluid viscosities are always highly mismatched.

Despite these differences, the structures observed (Fig. S2, ESI†) are strongly analogous to those seen in liquid/liquid/ particle systems. First, when the amount of liquid is very small, pendular structures appear (Fig. S2a, ESI†). Indeed, of all ternary liquid/fluid/particle systems, this may be the most familiar, since sandcastles are constructed from wet sand with precisely this pendular microstructure. Second, when there is sufficient fluid to engulf the particles, capillary aggregates appear. A particular type of capillary aggregate, called a spherical agglomerate, is shown in Fig. S2b (ESI†). Third, if the liquid is somewhat non-wetting towards the particles, then particle-stabilized foams, which are analogous to Pickering emulsions (except that the dispersed phase is air) can be prepared (Fig. S2d, ESI†). Finally, if the liquid is highly non-wetting towards the particles, powdered liquids (Fig. S2e also known as dry liquids, ESI†) can be created. These unusual materials, which consist of free-flowing granules of particle-coated liquid, are also analogous to

Pickering emulsions except that the continuous fluid is air. Individual granules are called liquid marbles, Fig. S2e (ESI†).

4. State diagram

The Introduction proposed that the consistent behavior of diverse systems is attributable to certain universal considerations that apply to all liquid/fluid/particle mixtures. To illustrate this idea, this section will construct a state diagram for ternary mixtures under some simplifying assumptions. Fig. 3 illustrates three representative slices of this state diagram, Fig. 3a at fixed particle loading of $\phi_p = 0.1$, and Fig. 3a and b at constant wettability. Fig. 3 has been drawn assuming that the particles are nearly hard spheres (not necessarily monodisperse), and assuming various symmetries, e.g. that the fluids have equal viscosity, or that the state diagram in the
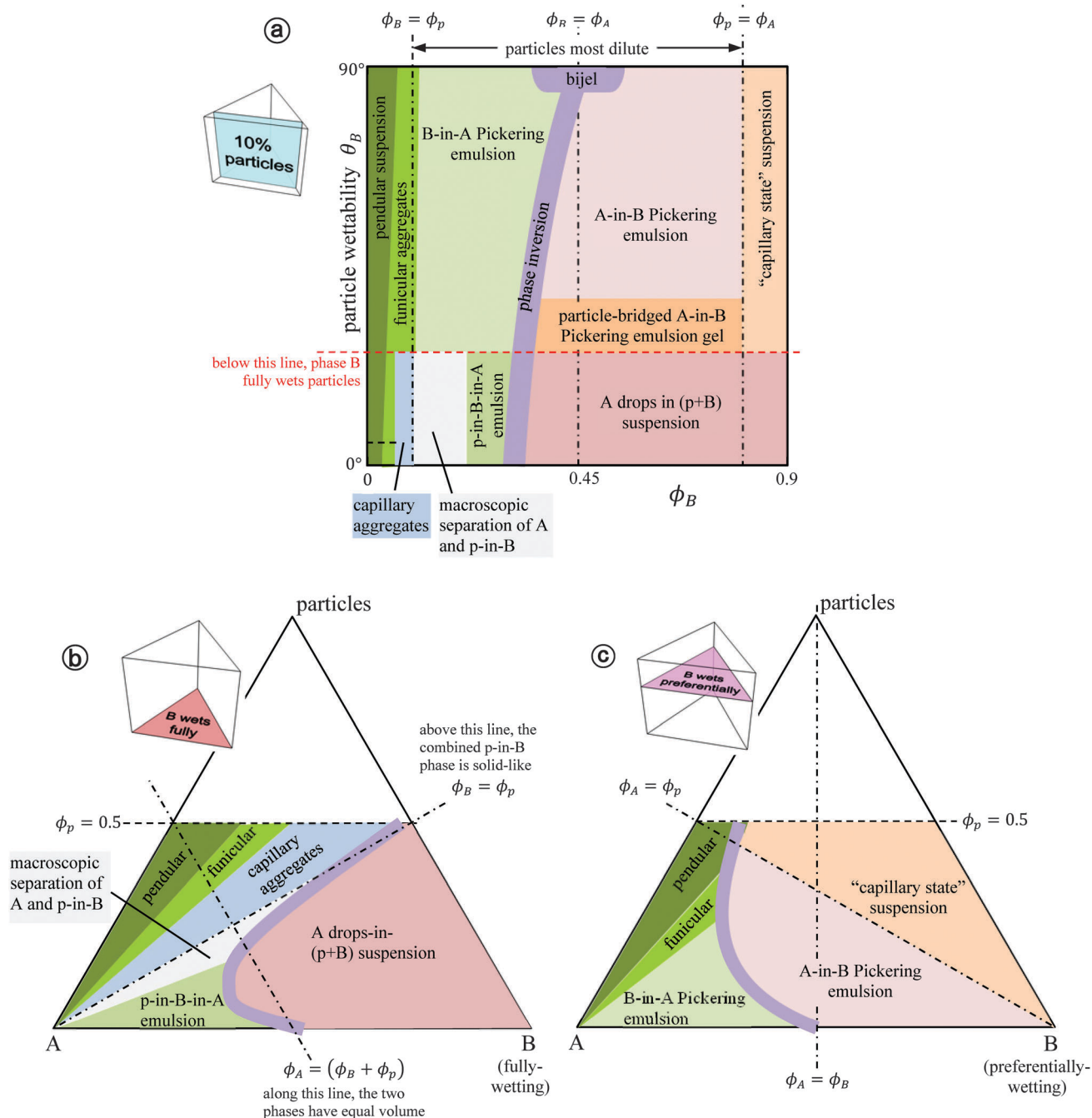

Fig. 3 State diagram represented in various cross sections (illustrated in the inset of each figure) of the triangular prism. Note that only the θ range from 0° to 90° is shown, and hence fluid B fully or partially wets the particles. (a–c) Show three cross sections of the prism (a) at fixed particle volume fraction of $\phi_p = 0.1$, (b) at fixed θ near zero so that that B fully wets the particles, and (c) at fixed θ such that B wets the particles preferentially, but not fully. The various structures noted are illustrated schematically in Fig. 2.

upper half of the prism is simply an inverted version of that in the lower half. Accordingly, only one half of the diagram with $\theta \leq 90°$ (*i.e.* B is fully- or preferentially-wetting) is illustrated. In Fig. 3b and c, the triangular region with $\phi_p > 0.5$ has been left unclassified for reasons discussed in Section 2. As in Section 3, we will first discuss mixtures in which particles are fully-wetted by both phases, followed by partially-wetting situations.

4.1. Fully-wetted particles

The fully-wetting situation corresponds to Fig. 3b and the lower portions of Fig. 3a (below the dashed red line). In this case, if there is sufficient amount of B to engulf most of the particles, the particles and B form a combined p-in-B phase with a total volume fraction of $(\phi_B + \phi_p)$ and a particle loading of $\phi_p^{eff} = \dfrac{\phi_p}{\left(\phi_B + \phi_p\right)}$. If ϕ_p^{eff} is small, then the combined phase is a dilute suspension with liquid-like rheology. With increasing ϕ_p^{eff}, the combined phase becomes increasingly viscous until at $\phi_p^{eff} \sim 0.5$, (or equivalently $\phi_B = \phi_p$, marked by a dot-dashed line in Fig. 3b) the combined phase is expected to become solid-like or glassy. On the other hand, if $\phi_B \ll \phi_p$, there is not sufficient wetting fluid to form a combined p-in-B phase. In that case a pendular state is realized.

In the pendular state (Fig. 2a and Fig. S2a, S3 and S4, ESI†), a meniscus of fluid B joins together two particles. The negative mean curvature of the wetting meniscus induces a pairwise interparticle adhesion force, $2\pi\gamma R_p$, where γ is the interfacial tension between the two liquids and R_p is the particle radius. For $R_p < 100$ μm, under most conditions, the pendular capillary force dominates over inertia, friction, or gravity,[24] and leads to the formation of pendular aggregates of multiple particles. For particle loadings exceeding a few percent, these aggregates are linked into a space-spanning network, *i.e.* the volume fraction for percolation of a pendular network is only a few percent.[12] Incidentally, wet granular materials, *e.g.* wet sand, constitute a special case where the particle volume fraction is over 50% – far exceeding percolation.

When the volume of the fully-wetting fluid increases to roughly 15–25% of the particle volume, the menisci start coalescing.[25] The capillary force is no longer pairwise, but involves multiple particles held together by a single fluid drop, sometimes called a funicular aggregate (Fig. 2a). Thus $\phi_B = 0.25\phi_p$ is chosen to mark the boundary between the pendular and the funicular state in Fig. 3b.

Upon further increase in ϕ_B, there is eventually sufficient fluid to engulf at least some particles completely. Thus funicular aggregates gradually transition to capillary aggregates (Fig. 2b and Fig. S3 and S4, ESI†) in which some particles are fully engulfed, whereas others continue to protrude out of the wetting fluid.[25] Based on literature on wet granular systems[26] (where $\phi_p \sim 0.6$), and our own observations at much lower particle loadings,[12] we set $\phi_B = 0.5\phi_p$ as the condition for this transition. Capillary aggregates are highly stable against changes in size. They cannot break readily because ϕ_p^{eff} significantly exceeds 0.5, and hence the combined p-in-B phase is strongly solid-like.

Furthermore, they cannot coalesce readily: even if two aggregates contact each other, the protruding particles hinder direct contact between their fluid regions. Since the aggregates can neither break nor coalesce readily, their size strongly depends on mixing history.[27] Such capillary aggregate formation is the basis of a process called wet granulation (or oil agglomeration in the coal industry[28]) in which particles in a less wetting fluid or in air are agglomerated into large tight clusters by addition of a fully-wetting fluid.[29] Due to repeated mutual collisions in a tumbler, the aggregates tend to have almost perfectly round shapes (Fig. S2b, ESI†), and hence this same process is sometimes called spherical agglomeration.[30] Finally, Fig. S4, ESI† shows that the capillary aggregates can sometimes themselves be fused into a space-spanning network, even at particle loadings as low as 10%.[12] This is because they can undergo partial coalescence, *i.e.* the liquid portion of two aggregates can merge, but the entire aggregate cannot recover a round shape since the capillary forces are insufficient to overcome the internal yield stress.[31]

When ϕ_B increases further, the p-in-B combined phase is no longer strongly solid-like, and moreover the fluid can now fully engulf all the particles, *i.e.* the particles no longer protrude out. For both these reasons, complete coalescence of aggregates becomes possible. The author has set $\phi_p^{eff} < 0.5$ as a condition for complete coalescence; depending on details such as polydispersity or minor interparticle attractions, a slightly higher or lower value of ϕ_p^{eff} may be equally justified. The condition $\phi_p^{eff} < 0.5$ is equivalent to $\phi_B > \phi_p$; thus, on the right of the lines marked $\phi_B = \phi_p$ in Fig. 3a and b, capillary aggregates are destroyed by coalescence. Yet, ϕ_p^{eff} is still very high (0.4–0.5), and therefore rheologically, the combined dispersed is still not fully liquid-like: it may have a weak yield stress, or at least a very high internal viscosity. Accordingly, although coalescence is possible, p-in-B aggregates cannot be broken readily under mixing conditions. This combination – aggregates that can coalesce, but not break – is a recipe for unbounded growth of the size of the dispersed phase. Consequently, macroscopic phase separation occurs: the combined p-in-B phase separates completely from the non-wetting A phase. In low viscosity mixtures in which gravity dominates,[11,26,30] this is manifested as a complete separation into stratified layers under quiescent conditions (Fig. 2c and Fig. S5 and S6e, ESI†). In high viscosity systems such as molten polymers where buoyancy is weak, this is manifested as a large increase in the size of the dispersed phase (Fig. S4, ESI†), perhaps to dimensions set by the geometry of the mixer.[11,27]

With further increase in ϕ_B the combined p-in-B dispersed phase becomes dilute in particles (ϕ_p^{eff} reduces), and therefore becomes capable of both breakup and coalescence like "normal" liquid-like drops. Accordingly, one should expect a p-in-B-in-A particles-in-drops structure (Fig. 2d and Fig. S6d and S8a, ESI†). In reality, such a structure is easy to see only at relatively low particle loading. It may not appear at all at high particle loading for two reasons. First, in low viscosity systems, *e.g.* oil/water, sedimentation is rapid, and the particle-containing drops can rapidly coalesce into separate layers, *i.e.*

even if the particles-in-drops structure is actually present *during* mixing conditions, it may not survive even for short durations *after* mixing. Second, the particles-in-drops structure requires liquid-like rheology within the drops, *i.e.* $\phi_B > \phi_p$. If the particles themselves are concentrated, the volume fraction of the combined dispersed phase would be fairly large, *e.g.* if $\phi_p = 0.3$, then $(\phi_B + \phi_p)$ would exceed 0.6. At such a high volume fraction, the combined p-in-B phase may not even remain the dispersed phase any more: *i.e.* as drawn in Fig. 3b, phase inversion may preempt the particles-in-drops structure.

Regardless of whether a particles-in-drops structure appears or not, with increasing ϕ_B, eventual phase inversion is inevitable. If the particles were truly fully-wetting towards B, one would expect that the particles and drops of A would be independently suspended in the B phase. However, often, even particles that can be engulfed by the B phase can nevertheless adsorb at the interface weakly, and therefore stabilize Pickering drops of A. Thus, when the wetting fluid B is the continuous phase, one likely obtains a mixture of particles and particle-stabilized A drops (Fig. 2e).

Finally, we comment on why phase inversion is shown to have a non-monotonic composition-dependence in Fig. 3b. Even in the ideal case when the particles are fully-wetted and have no interfacial effects, addition of particles induces two competitive effects. The first is volumetric mismatch: if particles are added keeping the A : B ratio fixed, the combined volume fraction, $(\phi_B + \phi_p)$ increases. Thus, a simple view that in a surfactant-free system, phase inversion occurs when the two phases have roughly equal volume would suggest that phase inversion follows the dot-dashed line labeled $\phi_A = (\phi_B + \phi_p)$. The second effect is viscosity mismatch: as the particle loading increases, the viscosity of the combined phase increases, whereas that of phase A remains fixed. This viscosity mismatch remains modest as long as ϕ_p^{eff} is small, but increases sharply as ϕ_p^{eff} approaches 0.5. It is well-recognized that when mixing two homogeneous fluids of mismatched viscosity, the phase with the high viscosity tends to become the dispersed phase even if it has a high volume fraction,[32] *i.e.* as ϕ_p increases beyond a few percent, a decreasing A : B ratio is needed for phase inversion. These two competing trends are qualitatively sufficient to cause non-monotonic behavior of the phase inversion composition. In fact, there is a third effect due to the fact that even particles that can be fully-engulfed may still have some interfacial activity. This interfacial effect will be discussed in Section 4.2, but here we only note that it acts in the same direction as the volumetric mismatch effect (*i.e.* tends to push the phase inversion in Fig. 3b to the left).

Two special cases deserve additional comment. The first is to reiterate that in polymeric systems where bulk viscosity is high, bicontinuous structures may appear near phase inversion, which are themselves flanked by regions where the dispersed phase appears highly elongated (Fig. S7 and S10, ESI†). Second, when one of the fluids is air, the inverted air-in-(p + B) structure (*i.e.* a foam) typically does not appear: usually bubbles rise rapidly and escape from the liquid phase (Fig. S2c, ESI†).

However, see ESI,† for comments on foams of particle-filled polymers.[33,34]

4.2. Partially-wetted particles

First consider the situation when the particles are dilute, and the preferentially-wetting fluid B is added to a p-in-A suspension (*i.e.* moving rightwards in the upper portion of Fig. 3a). The pendular state with pairwise menisci can still appear when $\phi_B \ll \phi_p$. For partially-wetted particles, the pairwise force $(2\pi R_p \gamma \cos \theta)$ becomes weaker as θ increases. Nevertheless, as long as the wetting angle is not too close to 90°, this pendular state is expected to resemble that discussed in Section 4.1. Furthermore, upon increasing ϕ_B, one may expect meniscus coalescence to lead to funicular clusters, again analogous to the previous section.

Beyond funicular clusters however, the similarity with the fully-wetted particles ends. For partially-wettable particles, the energy needed to desorb a single spherical particle from the interface into the preferentially-wetting phase is $\pi R_p^2 \gamma (1 - \cos \theta)^2$. Since this energy is typically many orders of magnitude larger than thermal energy $k_B T$, it is commonly accepted that particles adsorb irreversibly.[8] This is not strictly true: viscous, gravitational, or magnetic forces can pull particles off the interface. Nevertheless under many conditions, any particles that reach the interface during the mixing process tend to adsorb there indefinitely. Accordingly, upon further increasing ϕ_B, particles cannot be engulfed by the fluid B and capillary aggregates cannot appear; instead B-in-A Pickering emulsions appear (Fig. 2j). Since the particles are preferentially-wetted by B, these emulsions have particles protruding more onto the inside of the drops. This is not the favorable configuration as noted in Section 3.2 and in the ESI.† These emulsions directly invert into the more favorable A-in-B Pickering emulsions (Fig. 2h), with the particles protruding out of the drops. As ϕ_B continues increasing at fixed particle loading, eventually one reaches $\phi_p > \phi_A$, and it is no longer reasonable to think of this system as an emulsion. Instead, following the nomenclature of Koos *et al.*,[21,35] we may dub this a capillary state suspension in which particles are clustered together (Fig. 2g). Conceptually each cluster may be regarded as a Pickering emulsion drop where the fluid drop size is comparable to the size of a single particle. This state appears similar to the funicular state, except that here the particles are preferentially-wetted by the continuous phase. Once again, these clusters may be joined together into a percolating network, with individual particles being shared by two clusters.

Within this vertical slice, Fig. 3a, of the prism, two more special cases are noteworthy. The first is when the particles are strongly (but still not fully) wetted by the B phase, so that they protrude far outside the drops. In this case, the A-in-B emulsions may have the bridged Pickering emulsion gel structure (Fig. 2f and Fig. S15 and S16, ESI†).[36–38] This structure resembles the suspension in a capillary state, except that the drops are much bigger than the particles. It is noteworthy that the thin film of liquid B separating the drops is stable against thinning.[39] Second, when the particles are equally wetted by

both phases and if $\phi_A \sim \phi_B$, bijels (Fig. 2i and Fig. S17, ESI†) may be realized with appropriate preparation protocols. Bijels are often prepared by spinodal decomposition:[40,41] the system starts in a state when the two liquid phases are miscible, and then quenched to induce phase separation. During the phase separation and coarsening, particles adsorb at the interface at a sufficient coverage that interfacial jamming stabilizes the bicontinuous morphology. Very similar morphologies may also be prepared by simply melt-blending two polymers with particles.[42,43]

At higher particle loadings, *i.e.* far from the A–B edge in Fig. 3c, two qualitative changes are noteworthy. First, if the particles have a higher volume fraction than the drops, we dub the mixture a "suspension". Hence, simply as a matter of nomenclature, at large ϕ_p, more of the composition triangle is classified as a suspension in the capillary state rather than an A-in-B Pickering emulsion. Second, as noted in Section 3.2, favorable Pickering emulsions are ones in which the preferentially-wetting phase becomes the continuous phase even if it is a minority, *i.e.* the phase inversion line is asymmetric ($\phi_A > \phi_B$). This asymmetry is expected to increase with increasing ϕ_p *i.e.* the phase inversion curve moves left in Fig. 3c. Therefore at high particle loading, the B-in-A Pickering emulsion state may disappear altogether as drawn in Fig. 3c. The author is not aware of experimental data in this parameter space.

Finally, we discuss the factors governing phase inversion when particles are partially-wettable, most importantly why phase inversion (purple lines in Fig. 3a and c) occurs not when A and B have an equal volume, but instead when ($\phi_A > \phi_B$). The two competing effects, volumetric mismatch and viscosity mismatch, noted in Section 4.1 are both irrelevant here since the particles are not engulfed by the B phase. Thus, the particles affect phase inversion entirely *via* their interfacial activity. One possible mechanism is the effect of particles on drop coalescence. Particles that protrude out of the drops likely provide a greater steric hindrance to coalescence than those that protrude inwards. Indeed, the latter may even promote coalescence (see Fig. S6b, ESI†) by a mechanism known as bridging-dewetting in the foams literature.[44,45] Thus, particles make coalescence asymmetric: B-in-A Pickering emulsions coalesce much more readily than A-in-B Pickering emulsions. A long-proposed idea in the emulsion literature[46] states that the phase that becomes continuous is the one that coalesces faster. As per this idea, the asymmetric coalescence biases phase B to be the continuous phase. This may be one mechanism underlying the asymmetric nature of the phase inversion line.

Yet, the preference for the more wetting phase to be continuous appears even when the ternary mixture is prepared not by active mixing, but by quenching from the single-phase region (Fig. S14, ESI†) – a process which does not involve coalescence, but instead the fragmentation of an approximately-bicontinuous morphology resulting from spinodal decomposition. Here an alternate mechanism of "preferred interfacial curvature" may be invoked: since the particles adsorb asymmetrically on the interface, they bias the interface towards a curvature that can only be achieved when the preferentially-wetted phase is continuous.[47]

We close this section with comments on the special case when one phase is air and the particles are partially-wetting.

As mentioned in Section 3.3, several structures (pendular and funicular aggregates, and powdered liquids and foams) are broadly analogous to those seen in corresponding liquid systems. However, to the author's knowledge, bijels or other bicontinuous morphologies have never been noted when one phase is a gas.

5. Caveats and conclusions

Any attempt to impose "universality" onto real-world systems is fraught with complications and it is worthwhile noting some factors that are likely to cause deviation from Fig. 3. Foremost is the importance of processing history. As with all far-from-equilibrium systems, the structure results from a specific preparation protocol, and changing the preparation method may move the boundaries at which the structural transitions of Fig. 3 appear. A key aspect of the processing history is the strength of mixing. Fig. 4 illustrates the situation where $\phi_p < \phi_B \ll \phi_A$, *i.e.* both dispersed phases are dilute. When the particles are fully-wetted by B, a particles-in-drops structure is expected. However, it is immediately apparent that depending on the size of the drops relative to particles, one may realize the various situations illustrated in Fig. 4a: at one extreme, each drop of fluid B contains numerous particles whereas at the other extreme, many of the drops are freely-suspended in the continuous phase and not associated with the particles at all. Mixing intensity also affects the morphology when the particles are partially-wetted by both phases: at low mixing intensity (Fig. 4b left), one expects highly non-spherical structures with interfacially-jammed particles, whereas at higher intensity (Fig. 4b middle), the dispersed phase would have much smaller aspect ratio. Both these are interfacially-jammed, *i.e.* the total liquid–liquid interfacial area is simply what is needed to accommodate all the particles at the interface, yet, the different flow conditions produce a completely different aspect ratio. Fig. S21, ESI† shows a dramatic example of exactly such a morphological change due to varying flow conditions. At even higher mixing intensity (Fig. 4b right), one may expect the
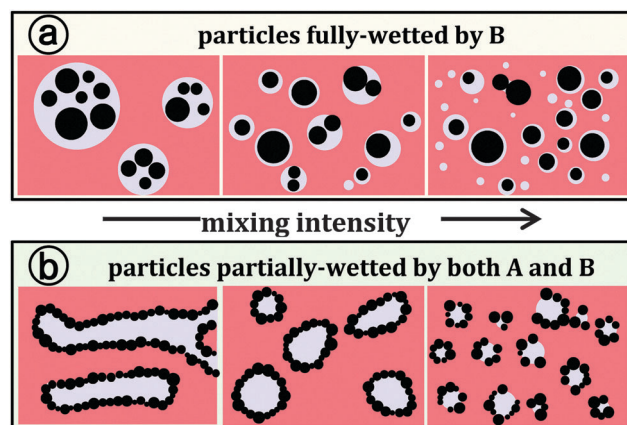

Fig. 4 Schematic of how mixing intensity affects structure when (a) particles are fully-wetted by phase B (shown in light blue), and (b) when particles are partially-wetted by both phases.

dispersed phase to become spherical and no longer interfacially-jammed, *i.e.* the viscous stresses are now able to generate more interfacial area than needed to accommodate the particles. In both Fig. 4a and b, the key effect of changing mixing conditions is to change the size of drops relative to particles. In a particle-free liquid/liquid mixture, the size of drops (or more generally, the lengthscale of the two-phase structure) is determined by the balance between viscous and interfacial forces. The lengthscale that emerges from this balance is γ/σ, where σ is the viscous stress associated with mixing. This lengthscale can then be used to define a capillary number based on particle size, $Ca_p = \sigma R_p/\gamma$. The author proposes that the effect of mixing intensity may be captured in terms of such a capillary number: mixing processes with $Ca_p \ll 1$ will produce qualitatively different morphologies from those with $Ca_p \gg 1$.

Another aspect of processing history is the sequence in which the three components are mixed. If particles are pre-dispersed in one phase *vs.* the other, there may be significant changes in the morphology,[48–50] presumably because the wettability of the particles depends on which fluid the particles contact first. In this situation, different processing conditions may be regarded as exploring different vertical positions in the triangular prism, *i.e.* exploring different wettabilities within the same state diagram.

A second significant complication is the effect of interparticle interactions and particle shape. With fully-wetting particles, familiar interactions such as DLVO or adsorbed polymer chains bridging across particles may significantly change the bulk rheology of the wetting phase. Most importantly, if the particles induce selective gelation of the fully-wetting fluid, it will likely expand the composition-space within which capillary aggregation or macroscopic phase separation appears. This issue has not been studied systematically, although the particle-filled polymer blends literature clearly recognizes that even very low particle loadings can greatly modify the morphology of the blend due to selective gelation of the wetting phase. Fig. S9 and S10, ESI† provide excellent examples of this. With partially-wetting particles, interfacially-located particles are known to attract each other due to capillary forces.[51] Van der Waals forces would further add to the attraction and form a mechanically-robust layer at the interface. Such interfaces are no longer liquid-like, but have strongly solid-like properties including non-zero inter-facial modulus and strength. Moreover, once the particles are in direct contact, interparticle friction may further accentuate the solid-like properties of the interface. These interfacial viscoelastic properties can greatly affect the stability of Pickering emulsions, and especially of interfacially-jammed structures such as non-spherical drops or bijels. These complexities will be accentuated if the particles are non-spherical since high aspect ratio particles can induce gelation at low particle loading if fully-wettable, and experience strong capillary attractions if adsorbed at the interface.[31,52] Indeed Fig. 3 may already be biased by these complexities since at least some of literature informing Fig. 3 used fumed silica particles which are notoriously complex: they induce gelation at low particle loading, have non-spherical fractal-like shapes, and can display hysteresis in wettability.

It must be emphasized that none of the transitions noted in this paper are sharp. Some transitions are a matter of nomenclature, *e.g.* in Fig. 3, an A-in-B Pickering emulsion is distinguished from the capillary state suspension simply based on which dispersed species is in a majority. Analogously, funicular aggregates and capillary state suspensions are distinguished only by whether the drops preferentially wet the particles or not – a distinction that loses meaning when the contact angle is near 90° degrees. Some transitions, *e.g.* pendular to funicular to capillary aggregate, occur continuously as composition is changed. Even phase inversion is not necessarily a sharp transition; it can sometimes occur *via* an intermediate fully-separated state (Fig. S5, ESI†) or *via* an intermediate bicontinuous state (Fig. S7, ESI†). Thus, all the transitions lines marked in Fig. 3 are better regarded as bands in which large changes in structure are expected.

The locations of these transitions are expected to shift somewhat from one system to another due to differences in mixing history, interparticle interactions, relative viscosity of the phases, particle roughness or polydispersity. However, even if the specific assumptions of Fig. 3 are not true, many of the underlying considerations that determine the transitions still remain true and can be invoked to predict the transition locations. For instance, the transition from pendular to capillary aggregates is almost entirely governed by the geometry of meniscus coalescence, and hence particle shape is expected to strongly affect this transition, but interparticle attractions will likely have only modest effects. In contrast, the transition from capillary aggregates to macrophase separation is governed by the particle loading at which the fully-wetted phase becomes solid-like, and hence is likely to be affected by both particle shape and interparticle attractions. By taking account of such specific considerations, one may draw state diagrams that apply to a narrower set of ternary mixtures. This is analogous to the literature in surfactant-oil-water systems: Fig. S1b (ESI†) applies generically, whereas more narrowly-tailored diagrams may be drawn for specific surfactant families.

In summary, while Fig. 3 is an idealized map, it is underpinned by broadly-applicable phenomena, and hence the qualitative features of Fig. 3 will likely be preserved in most liquid/fluid/particle systems. Liquid/fluid/particle mixtures have already led to new materials, either in their own right (*e.g.* filled polymer blends, powdered liquids, particle-stabilized foams), or as templates for further processing (*e.g.* colloidosomes,[53] bijel capsules[54]). The concept of a non-equilibrium state diagram provides a powerful framework to guide material selection, and formulate composition and processing conditions so that new materials with the desired morphologies can be realized. For instance, a formulation engineer who sees Pickering emulsions being unstable due to particle desorption into phase B may choose to move to a higher cross section of the prism where the particle-in-drops morphology transitions to a Pickering emulsion. This may require surface modification of particles, or it may be as simple as pre-dispersing the particles in fluid A so that B is no longer fully-wetting, *i.e.* taking advantage of the dependence of wettability on mixing history.

As a second example, one may seek to create networks based on partially-coalesced capillary aggregates. Fig. 3b suggests that adding particles to an A-in-B emulsion is less likely be successful since the structure may be trapped in a macroscopically-separated state Instead gradually adding phase B to a particles-in-A suspension is more likely to be successful.[27]

Finally monodisperse particles deserve special mention. This paper presumed that the particles were polydisperse. In fact some of the data informing Fig. 3 did use monodisperse particles, but these systems produced results similar to those with polydisperse particles. Yet, qualitatively new phenomena – specifically crystalline-ordered morphologies – may appear with monodisperse particles. Monodisperse particles suspended in a single liquid can crystallize, especially if flow is applied.[55,56] If the suspending medium comprises two immiscible liquids, then crystallization must accommodate the additional need to satisfy the desired contact angle, and to minimize liquid/liquid interfacial area. How particle crystallization proceeds when flow, wettability, and capillarity are coupled will provide a fertile area in soft materials research.

Acknowledgements

References

1 M. Kahlweit and R. Strey, Phase Behavior of Ternary Systems of the Type H₂O-Oil-Nonionic Amphiphile (Microemulsions), *Angew. Chem., Int. Ed. Engl.*, 1985, **24**(8), 654–668.

2 H. T. Davis, Factors determining emulsion type: Hydrophile—lipophile balance and beyond, *Colloids Surf., A*, 1994, **91**, 9–24.

3 M. S. Leaver, U. Olsson, H. Wennerstrom, R. Strey and U. Wurz, Phase-behavior and structure in a nonionic surfactant-oil-water mixture, *J. Chem. Soc., Faraday Trans.*, 1995, **91**(23), 4269–4274.

4 C. Ceschin, J. Roques, M. C. Maletmartino and A. Lattes, Fluorocarbon microemulsions, *J. Chem. Technol. Biotechnol., Chem. Technol.*, 1985, **35**(2), 73–82.

5 J. H. Lee, *et al.* Phase behavior of highly immiscible polymer blends stabilized by a balanced block copolymer surfactant, *Macromolecules*, 2003, **36**(17), 6537–6548.

6 M. A. Hillmyer, W. W. Maurer, T. P. Lodge, F. S. Bates and K. Almdal, Model bicontinuous microemulsions in ternary homopolymer block copolymer blends, *J. Phys. Chem. B*, 1999, **103**(23), 4814–4824.

7 N. R. Washburn, T. P. Lodge and F. S. Bates, Ternary polymer blends as model surfactant systems, *J. Phys. Chem. B*, 2000, **104**(30), 6987–6997.

8 B. P. Binks, Particles as surfactants – similarities and differences, *Curr. Opin. Colloid Interface Sci.*, 2002, **7**(1–2), 21–41.

9 S. Sacanna, W. K. Kegel and A. P. Philipse, Thermodynamically stable pickering emulsions, *Phys. Rev. Lett.*, 2007, **98**(15), 158301.

10 S. Nagarkar and S. S. Velankar, Rheology and morphology of model immiscible polymer blends with monodisperse spherical particles at the interface, *J. Rheol.*, 2013, **57**(3), 901–926.

11 S. J. Heidlebaugh, T. Domenech, S. V. Iasella and S. S. Velankar, Aggregation and Separation in Ternary Particle/Oil/Water Systems with Fully Wettable Particles, *Langmuir*, 2014, **30**(1), 63–74.

12 T. Domenech and S. S. Velankar, On the rheology of pendular gels and morphological developments in paste-like ternary systems based on capillary attraction, *Soft Matter*, 2015, **11**(8), 1500–1516.

13 Y. Nonomura and N. Kobayashi, Phase inversion of the Pickering emulsions stabilized by plate-shaped clay particles, *J. Colloid Interface Sci.*, 2009, **330**(2), 463–466.

14 E. Koos, Capillary suspensions: Particle networks formed through the capillary force, *Curr. Opin. Colloid Interface Sci.*, 2014, **19**(6), 575–584.

15 R. Mohammadi and A. Amirfazli, Contact angle measurement for dispersed microspheres using scanning confocal microscopy, *J. Dispersion Sci. Technol.*, 2004, **25**(5), 567–574.

16 M. Preuss and H. J. Butt, Measuring the contact angle of individual colloidal particles, *J. Colloid Interface Sci.*, 1998, **208**(2), 468–477.

17 L. Isa, F. Lucas, R. Wepf and E. Reimhult, Measuring single-nanoparticle wetting properties by freeze-fracture shadow-casting cryo-scanning electron microscopy, *Nat. Commun.*, 2011, **2**, 438.

18 M. Destribats, *et al.* Pickering Emulsions: What Are the Main Parameters Determining the Emulsion Type and Interfacial Properties?, *Langmuir*, 2014, **30**(31), 9313–9326.

19 D. E. Tambe and M. M. Sharma, Factors Controlling the Stability of Colloid-Stabilized Emulsions.1. An Experimental Investigation, *J. Colloid Interface Sci.*, 1993, **157**(1), 244–253.

20 B. P. Binks and J. H. Clint, Solid wettability from surface energy components: Relevance to pickering emulsions, *Langmuir*, 2002, **18**(4), 1270–1273.

21 E. Koos and N. Willenbacher, Capillary Forces in Suspension Rheology, *Science*, 2011, **331**(6019), 897–900.

22 C. Snoeyink, S. Barman and G. F. Christopher, Contact Angle Distribution of Particles at Fluid Interfaces, *Langmuir*, 2015, **31**(3), 891–897.

23 J. Shang, M. Flury, J. B. Harsh and R. L. Zollars, Comparison of different methods to measure contact angles of soil colloids, *J. Colloid Interface Sci.*, 2008, **328**(2), 299–307.

24 D. Schulze, Fundamentals, *Bulk Solids: Behavior, Characterization, Storage and Flow*, 2008, ch. 2, Springer, Berlin.

25 C. L. Flemmer, On the regime boundaries of moisture in granular materials, *Powder Technol.*, 1991, **66**(2), 191–194.

26 W. Pietsch, Tumble/growth agglomeration, *Agglomeration Processes: Phenomena, Technologies, Equipment*, 2008, ch. 7, Wiley, Weinheim.

27 T. Domenech and S. Velankar, Capillary-driven percolating networks in ternary blends of immiscible polymers and silica particles, *Rheol. Acta*, 2014, **53**(8), 1–13.

28 C. E. Capes and K. Darcovich, A survey of oil agglomeration in wet fine coal processing, *Powder Technol.*, 1984, **40**(1–3), 43–52.

29 W. Pietsch, *Agglomeration Processes: Phenomena, Technologies, Equipment*, 2008, Wiley, Weinheim.

30 A. F. Sirianni, C. E. Capes and J. E. Puddington, Recent experience with the spherical agglomeration process, *Can. J. Chem. Eng.*, 1969, **47**(2), 166–170.

31 A. B. Pawar, M. Caggioni, R. W. Hartel and P. T. Spicer, Arrested coalescence of viscoelastic droplets with internal microstructure, *Faraday Discuss.*, 2012, **158**, 341–350.

32 D. R. Paul and J. W. Barlow, Polymer blends (or alloys), *J. Macromol. Sci., Rev. Macromol. Chem.*, 1980, **C18**, 109–168.

33 L. M. Chen, D. Rende, L. S. Schadler and R. Ozisik, Polymer nanocomposite foams, *J. Mater. Chem. A*, 2013, **1**(12), 3837–3850.

34 J. Lobos and S. S. Velankar, How much do nanoparticle fillers improve the modulus and strength of polymer foams?, *J. Cell. Plast.*, 2015, DOI: 10.1177/0021955X14546015.

35 E. Koos and N. Willenbacher, Particle configurations and gelation in capillary suspensions, *Soft Matter*, 2012, **8**(14), 3988–3994.

36 S. P. Nagarkar and S. S. Velankar, Morphology and rheology of ternary fluid-fluid-solid systems, *Soft Matter*, 2012, **8**(32), 8464–8477.

37 T. S. Horozov and B. P. Binks, Particle-stabilized emulsions: A bilayer or a bridging monolayer?, *Angew. Chem.*, 2006, **45**(5), 773–776.

38 M. N. Lee, H. K. Chan and A. Mohraz, Characteristics of Pickering Emulsion Gels Formed by Droplet Bridging, *Langmuir*, 2012, **28**(6), 3085–3091.

39 N. D. Denkov, I. B. Ivanov, P. A. Kralchevsky and D. T. Wasan, A possible mechanism of stabilization of emulsions by solid particles, *J. Colloid Interface Sci.*, 1992, **150**(2), 589–593.

40 M. E. Cates, R. Adhikari and K. Stratford, Colloidal arrest by capillary forces, *J. Phys.: Condens. Matter*, 2005, **17**(31), S2771–S2778.

41 E. M. Herzig, K. A. White, A. B. Schofield, W. C. K. Poon and P. S. Clegg, Bicontinuous emulsions stabilized solely by colloidal particles, *Nat. Mater.*, 2007, **6**(12), 966–971.

42 K. Cheah, M. Forsyth and G. P. Simon, Processing and morphological development of carbon black filled conducting blends using a binary host of poly(styrene co-acrylonitrile) and poly(styrene), *J. Polym. Sci., Part B: Polym. Phys.*, 2000, **38**(23), 3106–3119.

43 M. Sumita, K. Sakata, S. Asai, K. Miyasaka and H. Nakagawa, Dispersion of fillers and the electrical conductivity of polymer blends filled with carbon black, *Polym. Bull.*, 1991, **25**, 266–271.

44 P. R. Garrett, Mode of action of antifoams, in *Defoaming*, ed. P. R. Garrett, 1993, Marcel Dekker, New York.

45 P. Thareja, K. Moritz and S. S. Velankar, Interfacially active particles in droplet/matrix blends of model immiscible homopolymers: Particles can increase or decrease drop size, *Rheol. Acta*, 2010, **49**(3), 285–298.

46 J. T. Davies, A quantitative kinetic theory of emulsion type. I. Physical chemistry of the emulsifying agent, *Gas/Liquid and Liquid/Liquid Interfaces, Proceedings of the International Congress of Surface Activity*, 1957, Butterworths, London, pp. 426–438.

47 P. A. Kralchevsky, I. B. Ivanov, K. P. Ananthapadmanabhan and A. Lips, On the thermodynamics of particle-stabilized emulsions: Curvature effects and catastrophic phase inversion, *Langmuir*, 2005, **21**(1), 50–63.

48 L. Elias, F. Fenouillot, J. C. Majeste, G. Martin and P. Cassagnau, Migration of nanosilica particles in polymer blends, *J. Polym. Sci., Part B: Polym. Phys.*, 2008, **46**(18), 1976–1983.

49 B. P. Binks and J. A. Rodrigues, Types of phase inversion of silica particle stabilized emulsions containing triglyceride oil, *Langmuir*, 2003, **19**(12), 4905–4912.

50 B. P. Binks and S. O. Lumsdon, Effects of oil type and aqueous phase composition on oil–water mixtures containing particles of intermediate hydrophobicity, *Phys. Chem. Chem. Phys.*, 2000, **2**(13), 2959–2967.

51 L. Botto, E. P. Lewandowski, M. Cavallaro and K. J. Stebe, Capillary interactions between anisotropic particles, *Soft Matter*, 2012, **8**(39), 9957–9971.

52 B. Madivala, S. Vandebril, J. Fransaer and J. Vermant, Exploiting particle shape in solid stabilized emulsions, *Soft Matter*, 2009, **5**(8), 1717–1727.

53 A. D. Dinsmore, *et al.* Colloidosomes: Selectively permeable capsules composed of colloidal particles, *Science*, 2002, **298**(5595), 1006–1009.

54 J. W. Tavacoli, J. H. J. Thijssen, A. B. Schofield and P. S. Clegg, Novel, Robust, and Versatile Bijels of Nitromethane, Ethanediol, and Colloidal Silica: Capsules, Sub-Ten-Micrometer Domains, and Mechanical Properties, *Adv. Funct. Mater.*, 2011, **21**(11), 2020–2027.

55 B. J. Ackerson, Shear induced order and shear processing of model hard sphere suspensions, *J. Rheol.*, 1990, **34**(4), 553–590.

56 Y. L. Wu, D. Derks, A. van Blaaderen and A. Imhof, Melting and crystallization of colloidal hard-sphere suspensions under shear, *Proc. Natl. Acad. Sci. U. S. A.*, 2009, **106**(26), 10564–10569.

57 X. X. Cai, B. P. Li, Y. Pan and G. Z. Wu, Morphology evolution of immiscible polymer blends as directed by nanoparticle self-agglomeration, *Polymer*, 2012, **53**(1), 259–266.

58 S. H. Lee, M. Bailly and M. Kontopoulou, Morphology and Properties of Poly(propylene)/Ethylene-Octene Copolymer Blends Containing Nanosilica, *Macromol. Mater. Eng.*, 2012, **297**(1), 95–103.

59 S. Tarimala and L. L. Dai, Structure of microparticles in solid-stabilized emulsions, *Langmuir*, 2004, **20**(9), 3492–3494.

60 B. P. Binks and S. O. Lumsdon, Catastrophic phase inversion of water-in-oil emulsions stabilized by hydrophobic silica, *Langmuir*, 2000, **16**(6), 2539–2547.